Macromolecules
ARTICLE

Macromolecules **2010**, *43*, 6099–6105 **6099**
DOI: 10.1021/ma100969j

Evaluation of Nematic Interaction Parameter between Polymer Segments and Low-Mass Molecules in Mixtures

Shogo Nobukawa, Osamu Urakawa,* Toshiyuki Shikata, and Tadashi Inoue

Department of Macromolecular Science, Graduate School of Science, Osaka University, 1-1 Machikaneyama-cho, Toyonaka, Osaka 560-0043, Japan

Received May 2, 2010; Revised Manuscript Received June 21, 2010

ABSTRACT: We conducted dynamic viscoelastic and birefringence measurements for dynamically homogeneous mixtures, polystyrene (PS)/4-pentyl-4′-cyanobiphenyl (5CB), to examine the orientational coupling between PS segments and 5CB molecules. It was also investigated whether dynamic homogeneity was correlated with orientational coupling. We determined stress-optical coefficients C_R of the PS/5CB mixtures in the rubbery region. With increasing the 5CB concentration, C_R increased indicating the cooperative orientation of the 5CB molecule along with the PS segment to some extent. We proposed a new method to quantitatively evaluate the orientational coupling, referred to as a nematic interaction (NI), between polymer segments and low-mass molecules in the mixtures from the concentration dependence of C_R. Using the proposed method we determined the NI parameter between PS and 5CB, $\varepsilon_{PS,5CB}$. The determined $\varepsilon_{PS,5CB}$ value was smaller than (about 1/4 of) that between PS segments ($\varepsilon_{PS,PS}$) suggesting the weaker NI acting between different chemical species with different shapes and sizes. Furthermore, this result means that dynamic homogeneity is not correlated with the value of a NI parameter.

1. Introduction

Thermal and mechanical properties of polymer/low-mass molecule (LM) mixtures, which have been widely studied so far,[1] are related to both polymer chain dynamics and LM dynamics. Glass transition temperature (T_g) of polymers decreases with the addition of LMs. This is well-known as the "plasticizing effect". Although both the segmental motion of polymers and the rotational motion of LMs are responsible for the glass transition phenomena, these two kinds of motion in polymer/LM mixtures are not completely cooperative. For example, polystyrene (PS)/toluene (Tol) mixtures exhibit two dielectric relaxation processes corresponding to the motions of PS-segments and Tol molecules in different temperature regions at a constant frequency.[2−4] Such a phenomenon is called "dynamic heterogeneity". However, in the case of larger LMs than Tol, for example, 4-pentyl-4′-cyanobiphenyl (5CB, Figure.1) fully miscibilized in PS, the rotational motion of 5CB is not distinct from the segmental motion of PS and thus these two dynamical processes are considered to be almost cooperative.[5−8] In other words, dynamic homogeneity of the PS/5CB blend is high. We speculated that this behavior was mainly due to the large molecular size of 5CB (1.3 nm) comparable with the segmental size of PS (1.9 nm).

Dynamic homogeneity (cooperative dynamics) of mixtures has been discussed based on the difference in the component relaxation times or friction coefficients at the segmental level including their temperature dependencies.[9−22] On the other hand, there is another cooperative phenomenon in miscible blends, i.e., local orientational coupling referred to as a nematic interaction (NI), which is observed as an enhancement of the optical anisotropy in applying the deformation on polymer materials. NI acts between the adjacent anisotropic molecules to be oriented in the same direction,[23−28] leading to the cooperative orientation between the components to some extent in mixtures. Naturally, the following question arises. "Is there a correlation between dynamical cooperativity (homogeneity) and orientational coupling in the mixtures?" We think that if strong NI acts between component species, the component dynamics will possibly become cooperative. However, strong NI will not necessarily be the origin of the cooperative dynamics since the dynamically homogeneous state just requires both components to have similar friction coefficients in the mixture and does not require local orientational coupling. In order to ascertain the truth of these considerations, we choose a PS/5CB blend as a model system, in which the component dynamics is known to be cooperative as mentioned before and compare the NI parameter of this mixture with the typical values of that reported for chemically identical polymer blends with different molecular weights.[28] (Strictly speaking, the components do not have the same chemical structure, since one component is deuterated.)

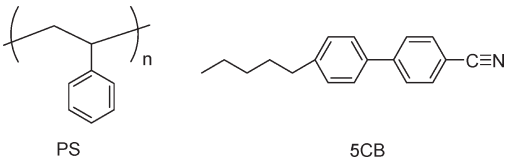

Figure 1. Chemical structures of polystyrene (PS) and 4-pentyl-4′-cyanobiphenyl (5CB).

For the evaluation of the NI effect, optical anisotropy measurements, such as birefringence and absorption dichroism, have been made so far,[26−28] based on the theory proposed by Doi et al.[23] for single component entangled polymers. Afterward, Zawada et al.[27] extended their theory to be applicable to binary polymer blends and determined the NI parameter in a miscible polyisoprene/poly(vinyl ethylene) blend. Concerning the NI in polymer/LM mixtures, there is no study as far as we know. In such blends, LM component does not contribute to the stress but does contribute to the birefringence through the NI in the rubbery-to-terminal region. Therefore, alternative theoretical formula is necessary to

*Corresponding author. E-mail: urakawa@chem.sci.osaka-u.ac.jp.

Published on Web 07/01/2010

determine the NI parameter in polymer/LM mixtures. In the theoretical section of this paper, we will propose a modified version of the Zawada's equation to be usable for the data analysis of such mixtures.

By taking the NI effect into account as well as from our previous experimental results about the PS/5CB blend described above,[5−8] the relaxation process of this blend can be considered as follows. In the glass to rubber transition zone, the externally imposed orientations of PS segments and 5CB molecules cooperatively and partially relax. At this stage a part of the orientation of 5CB molecules still remains on account of the NI with the partially oriented (unrelaxed) PS chains. In the rubbery to terminal region, the residual orientation of 5CB molecules disappears as the PS chain completely relaxes. Therefore, the NI parameter in PS/5CB blends can be estimated by evaluating the degree of orientation of each component in the rubbery or terminal region. In this study, we investigated the dynamic viscoelastic and birefringence behavior for PS/5CB mixtures and evaluated the magnitude of the orientational correlation (NI parameter) between PS segments and 5CB molecules in the rubbery region.

Tagaya and co-workers reported that polymer birefringence could be tuned to be zero by mixing a LM, such as a poly(methyl methacrylate)/stilbene system.[29] Saito and Inoue also reported that some miscible polymer blends became zero-birefringent by adjusting the component compositions.[30] In their studies, however, the effect of NI was not considered at all. In this paper, we want to emphasize the importance of the NI and the necessity to take into account it toward the control of the birefringence property of miscible blends.

2. Theoretical Background

2.1. Modified Stress-Optical Rule. Tensile strain, ε_t, induces the polymer chain orientation and consequently birefringence, Δn is observed. Δn is defined as the difference between two refractive indexes, $n_\parallel$ and $n_\perp$, in the directions parallel and perpendicular to the stretching direction.

$$\Delta n = n_\parallel - n_\perp \tag{1}$$

Generally, Δn is proportional to the tensile stress, σ, for homopolymer melts in the rubbery state, so-called stress-optical rule (SOR). The strain-optical coefficient, $O\,(=\Delta n/\varepsilon_t)$, is also proportional to Young's modulus, $E\,(=\sigma/\varepsilon_t)$, with the same proportional constant, C:

$$\Delta n = C\sigma, \quad O = CE \tag{2}$$

Here, C is called the stress-optical coefficient. In the glass-to-rubber transition region of polymeric materials, however, the SOR does not hold since the rubbery and glassy relaxation components have different stress-optical coefficients. Concerning this phenomenon, Inoue et al.[31−34] proposed a modified SOR (MSOR), i.e., the stress and birefringence can be described by the sum of two components, rubbery and glassy components (denoted by the subscripts R and G, respectively).

$$E^*(\omega) = E^*_R(\omega) + E^*_G(\omega) \tag{3}$$

$$O^*(\omega) = O^*_R(\omega) + O^*_G(\omega) = C_R E^*_R(\omega) + C_G E^*_G(\omega) \tag{4}$$

Here, $E^*(\omega)$ $(=E'(\omega) + iE''(\omega))$ is the complex Young's modulus and $O^*(\omega)$ $(=O'(\omega) + iO''(\omega))$ is the complex strain-optical coefficient. From $E^*(\omega)$ and $O^*(\omega)$ data, the $E^*_R(\omega)$ and $E^*_G(\omega)$ can be separately determined via eqs 3 and 4. C_R reflects the orientation of polymer chain (segment), and this value depends on the anisotropic polarizability of the repeat units of polymers. In contrast, C_G is related to the torsional orientation of the repeat units.[32−34]

2.2. Nematic Interaction and Stress-Optical Coefficient in Polymer/LM mixtures. Doi et al.[23] proposed the theory to account for NI in entangled polymer systems. Zawada et al.[27] extended their theory to apply to miscible binary polymer mixtures in which both components entangle. In this section, we propose a new equation to be applicable to polymer/LM system based on the Zawada's approach.

The orientation of the entanglement strands (of the length a) are characterized by orientation distribution S_{ij} (i or j stands for one of the direction, x, y, or z in the Cartesian coordinate) of the unit vector r_i ($i = x, y, z$) parallel to the vector connecting two adjacent entanglement points: $S_{ij} \equiv \langle r_i r_j - \delta_{ij}/3\rangle$, where δ_{ij} stands for the Kronecker δ. For an entangled polymer system, the deviatoric part of the stress tensor is related to the orientation distribution by

$$\sigma_{ij} = 3kT\frac{x}{N_e}S_{ij} \tag{5}$$

where k is the Boltzmann constant, T is absolute temperature, x is the number of freely jointed (Kuhn) bonds per unit volume, and N_e is the number of Kuhn bonds in the entanglement strand. On the other hand, refractive index tensor n_{ij} can be directly related to the local orientation distribution q_{ij} of the unit vectors u_i of the Kuhn bonds ($q_{ij} = \langle u_i u_j - \delta_{ij}/3\rangle$) through a coefficient corresponding to the intrinsic birefringence Δn_0:

$$n_{ij} = \Delta n_0 q_{ij} \tag{6}$$

This expression is different from that in ref 27 in order to be applied to polymer/LM blends.

According to Doi et al.,[23] orientational distribution of Kuhn bonds is affected by the surrounding orientational field due to nematic like interaction and two orientational distribution tensors for entangled polymers are related by the following equation.

$$q_{ij} = \frac{3l^2}{5{N_e}^2b^2}S_{ij} + \varepsilon q_{ij} \tag{7}$$

where b is the length of a Kuhn bond, l is the length measured along the primitive chain pass between two entanglement points or between two slip-links ($l = N_e b^2/a$) and ε ($0 \le \varepsilon \le 1$) is the nematic interaction parameter meaning the strength of the orientational coupling between a given probe polymer and its surroundings. The first term of the right-hand side in eq 7 represents the effect of slip-link constraints, and the second term the effect of orientational coupling. To simplify the equation, the term $3l^2/(5{N_e}^2b^2)$ is replaced by K and eq 7 is rewritten as

$$q_{ij} = \frac{1}{1-\varepsilon}KS_{ij} \tag{8}$$

Note that S_{ij} of LM component is considered to be zero since the LM size is generally smaller than entanglement strands and the vector r_i (connecting two entanglement points) of LMs cannot be defined. For polymer/LM (A/B) mixtures, eq 8 takes on more complicated forms due to coupling between different species (polymer and LM) as well as between the same species. Following the approaches of Doi et al.[23] and Zawada et al.,[27]

q_{ij} of the each component in polymer/LM mixture is given by

$$q_{ij,A} = K_A S_{ij,A} + \phi_A \varepsilon_{A,A} q_{ij,A} + \phi_B \frac{x_B}{x_A} \varepsilon_{A,B} q_{ij,B} \quad (9)$$

$$q_{ij,B} = \phi_B \varepsilon_{B,B} q_{ij,B} + \phi_A \frac{x_A}{x_B} \varepsilon_{B,A} q_{ij,A} \quad (10)$$

where the NI parameter, *e.g.*, $\varepsilon_{A,B}$ represents the coupling of component A with the orientational field of component B, and ϕ_A (or ϕ_B) is the volume fraction of component A (or B). It is noteworthy that eq 10 does not contain the S_{ij} term (corresponding to the slip-link constraint) and the orientation of LMs is affected only by the orientational coupling with both orientated polymer chains and LMs themselves.

From eq 6 and the additivity rule, the refractive index tensor of A/B mixture, $n_{ij,blend}$, may be expressed as

$$n_{ij,blend} = \phi_A \Delta n_{0,A} q_{ij,A} + \phi_B \Delta n_{0,B} q_{ij,B} \quad (11)$$

As for $\sigma_{ij,blend}$, only the polymer component generates the stress (LM does not contribute to the stress), and thus

$$\sigma_{ij,blend} = 3kT \frac{x_A}{N_{e,A}} \phi_A S_{ij,A} \quad (12)$$

From eqs 9∼12, following equation is obtained.

$$n_{ij,blend} = \left[\frac{1 + \dfrac{\phi_B \varepsilon_{B,A} \dfrac{\Delta n_{0,B}}{\Delta n_{0,A}} \dfrac{x_A}{x_B}}{(1 - \phi_B \varepsilon_{B,B})}}{1 - \phi_A \varepsilon_{A,A} - \dfrac{\phi_A \phi_B \varepsilon_{A,B} \varepsilon_{B,A}}{(1 - \phi_B \varepsilon_{B,B})}} C_A{}^0 \right] \sigma_{ij,blend} \quad (13)$$

Here $C_A{}^0$ is the stress-optical coefficient of pure A without nematic interaction and is related to the actual stress-optical coefficient C_A defined by eq 2 as

$$C_A{}^0 = (1 - \varepsilon_{A,A}) C_A \quad (14)$$

Equation 13 indicates that the stress-optical coefficient, C_R, of polymer/LM blends corresponding to the term in the bracket is a function of the composition, intrinsic parameters for pure components (Δn_0, x), and four NI parameters $\varepsilon_{A,A}$, $\varepsilon_{B,B}$, $\varepsilon_{A,B}$, and $\varepsilon_{B,A}$.

Intrinsic birefringence, Δn_0, corresponding to the birefringence for the perfectly oriented molecules to the stretching direction, is defined as $\Delta n_0 = \Delta n / P_2$, where P_2 is the orientation function and $P_2 = (3\langle \cos^2 \theta \rangle - 1)/2$, with θ being the angle between the molecular axis and the stretching direction. Apparent intrinsic birefringence $\Delta \tilde{n}_0$ of a polymer segment can be experimentally determined by the following equation,

$$\Delta \tilde{n}_0 = \frac{5}{3} O_R'(\infty) = \frac{5}{3} C_R E_R'(\infty) \quad (15)$$

Here, the factor 5/3 corresponds to ε/P_2 calculated under the assumption of pseudoaffine deformation with small amplitude[35,36] and $E_R'(\infty)$ is the limiting modulus of the rubbery component at high frequency, which can be estimated from the decomposed E_R' spectra. If there is no NI, $\Delta \tilde{n}_0$ becomes Δn_0. Therefore, Δn_0 of a single component polymer can be determined as ${}^5/_3 C_R{}^0 E_R'(\infty)$.

Table 1. Weight Fractions of 5CB and Glass Transition Temperatures for PS/5CB Blends

W_{5CB}	T_g (K)
0	368
0.05	359
0.13	335
0.20	316

From eqs 13 and 15, the apparent intrinsic birefringence of polymer/LM (A/B) mixtures $\Delta \tilde{n}_{0,blend}$ is written as

$$\Delta \tilde{n}_{0,blend} = \frac{\phi_A \left(\Delta n_{0,A} + \dfrac{\phi_B \varepsilon_{B,A} \Delta n_{0,B} x_A / x_B}{1 - \phi_B \varepsilon_{B,B}} \right)}{1 - \phi_A \varepsilon_{A,A} - \dfrac{\phi_A \phi_B \varepsilon_{A,B} \varepsilon_{B,A}}{1 - \phi_B \varepsilon_{B,B}}} \quad (16)$$

In the derivation of this equation, the relation of $E_{R,blend}'(\infty) = \phi_A E_{R,A}'(\infty)$, which is known to be valid for polymer/LM systems in the Rouse region (corresponding to the polymer chain motion inside the entanglement points) was used, because of the following reasons: all the observed data in this study were in the higher frequency region than the frequency where entanglement plateau appears, and the LM component (B) motion does not contribute to Young's modulus in the R-mode. In analyzing the data in the entanglement region, eq 13 must be used instead of eq 16. In this study we use eq 16 and examine the magnitude of the intercomponent NI parameter $\varepsilon_{B,A}$ or $\varepsilon_{A,B}$ (actually these two values are assumed to be the same) for PS/5CB mixtures.

3. Experimental Section

3.1. Materials. Polystyrene (PS) and 4-pentyl-4′-cyanobiphenyl (5CB) were purchased from Wako Chemicals. Their chemical structures are shown in Figure.1. PS was purified by reprecipitation of the PS/dioxane (good solvent) solution into ethanol (nonsolvent). 5CB was used as received. The weight-average-molecular-weight (M_w) and the molecular weight distribution index (M_w/M_n) of PS were 1.55×10^5 and 3.1, respectively. All blend samples were prepared by freeze-drying method from benzene solutions. The dried blend samples were pressed into sheets with the size of 25 mm ×5 mm ×1 mm at temperatures above T_g+50 K, for the dynamic viscoelastic and birefringence measurements.

Although 5CB is not volatile, we sometimes observed a little bit weight loss especially during the freeze-drying process. Therefore, the weight fractions of 5CB, W_{5CB}, of all the blends were determined by ^{1}H NMR measurement using EXcalibur-270 (JEOL Ltd., Tokyo, Japan) for the deuterated chloroform solutions in which the small portion of the dried blend film was dissolved. We checked NMR spectra of the samples after the viscoelastic and birefringence measurements and confirmed that W_{5CB} was constant during the measurements within the experimental error.

3.2. Methods. Dynamic viscoelastic and birefringence measurements were carried out with the oscillatory tensile rheometer (Rheospectoler DVE-3, Rheology Co. Ltd., Kyoto, Japan) equipped with the optical system at several temperatures between $T_g - 5$ K and $T_g + 30$ K in the frequency range of 1−130 Hz.

Differential scanning calorimeter (DSC EXSTAR-6000, Seiko Instruments Inc., Chiba, Japan) was operated to determine the glass transition temperature T_g for each blend. The value of T_g was estimated as the inflection point of the DSC trace for the glass transition process upon heating with the scan rate of 10 K/min. Values of T_g and W_{5CB} are summarized in Table 1.

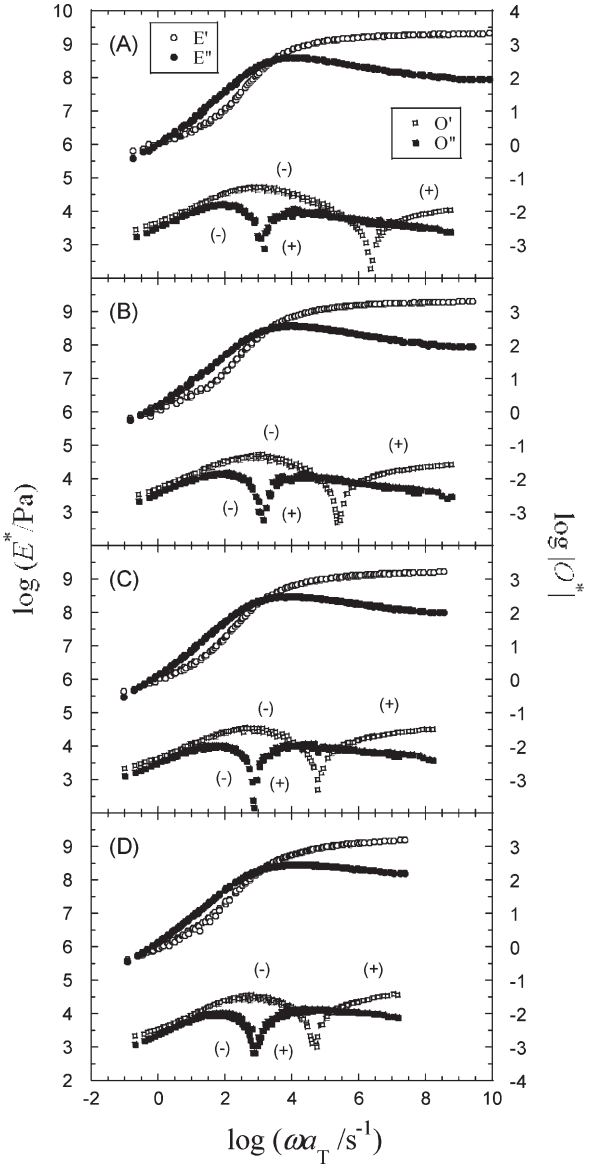

Figure 2. Master curves of complex elastic modulus, $E^* = E' + iE''$, and complex strain-optical coefficient, $O^* = O' + iO''$, for PS (A) and PS/5CB blends with $W_{5CB} = 0.05$ (B), 0.13 (C), and 0.20 (D) at reference temperatures, 348, 339, 315, and 296 K, respectively, which correspond to $T_g + 20$ K.

4. Results and Discussion

4.1. Viscoelastic and Birefringence Behaviors of PS and PS/5CB Blends. Figure 2 shows the composite curves of $E^*(\omega)$ and $O^*(\omega)$ for pure PS (A) and PS/5CB blends (B−D) at reference temperatures, $T_r = T_g + 20$ K. It is well-known that time−temperature superposition principle does not hold in the glass-to-rubber transition region of amorphous polymers.[37−39] Actually $E^*(\omega)$ and $O^*(\omega)$ data measured at different temperature were not superposable in a precise sense. However, in these figures, all the data were roughly superposed to see the global shapes of the $E^*(\omega)$ and $O^*(\omega)$ spectra. For the quantitative discussion, the master curves for separated E_R^* and E_G^*, which are superposable,[38,39] will be presented in the next section. The (+) and (−) symbols in Figure.2 represent the sign of O^* data. The different signs at high and low frequencies mean the relevant motional units are different at high and low frequencies since they should have different stress-optical coefficients.[31−34]

The shapes and locations of E^* curves are almost the same for all samples compared at $T = T_g + 20$ K (T_g varies 368−316 K for $W_{5CB} = 0$−0.2 as shown in Table 1). This means that the mechanical relaxation spectra of PS/5CB blends can be approximately regarded as a universal function of $T - T_g$. In contrast, O' spectra can be seen to depend on W_{5CB} especially in the position of the apparent valley of log O' curves where the sign in O' changes. The apparent minimum in the log O' curve shifts to the lower frequency side with increasing W_{5CB}. This is because the magnitude of O' of the blend in the glass-plateau region at the highest frequency slightly increases with W_{5CB} and the opposite signs at low and high frequency make such slight change visible. The increase of high-ω plateau in O' with W_{5CB} (corresponding to the increase of C_G as will be shown in Figure 5) is attributable to the higher intrinsic birefringence of 5CB than PS as will be discussed in sections 4.4 and 4.5.

4.2. Application of Modified Stress-Optical Rule. We think the breakdown of time−temperature superposition principle (TTS) in the transition region originates from different temperature dependencies of the two relaxation modes (rubbery and glassy modes). Inoue et al. showed that TTS holds for each mode.[38,39] As described previously, the two relaxation components can be separated into two modes based on MSOR (eqs 3 and 4) in principle at each temperature. First, we determined two stress optical coefficients C_R and C_G at the highest and at the lowest temperatures, respectively, where only the R or G mode was dominantly observed in both the stress and birefringence data. Thus, determined two coefficients were tentatively assumed to be independent of T. After reasonable separation into the two modes was attained for all the data at each temperature with temperature independent C_R and C_G, we assumed only the C_R is inversely proportional to T.[40,41]

$$C_R(T) = C_R(T')\frac{T'}{T} \tag{17}$$

Then, we reexamined the separation procedure and TTS for each mode with temperature-dependent C_R. As a result, it was found that the correction of C_R by eq 17 did not practically give significant change of the shapes of both E_R^* and E_G^* spectra as well as the shift factors. However, for the comparison of C_R values determined at widely separated temperatures, we judged this correction was necessary and used eq 17 for the application of the MSOR. On the other hand, C_G was assumed to be independent of T. The MSOR with temperature-dependent-C_R worked well for all the systems ($W_{5CB} = 0$−0.20).

After the separation of $E^*(\omega)$ data into the rubbery (E_R^*) and glassy (E_G^*) components at each temperature, master curves were constructed for each mode. The vertical shift for E_R^* was assumed to be proportional to T according to the rubber elasticity theory but as for E_G^* no vertical shift was applied. The results (master curves) are shown in Figure 3. TTS held for both modes of all the samples, indicating that dynamic heterogeneity (concerning the heterogeneity of the component dynamics[9−22]) is very low for these blends. This is consistent with our previous dielectric and viscoelastic results, i.e. the rotational motion of 5CB are coupled with the segmental relaxation of PS.[6−8] However, the shapes of E_R^* and E_G^* curves are slightly dependent on W_{5CB}: slight broadening of both spectra with increasing W_{5CB} is observed. This might be due to the concentration fluctuation effect.

The obtained shift factors of the R- and G- modes to construct the master curves are shown in Figure 4. The

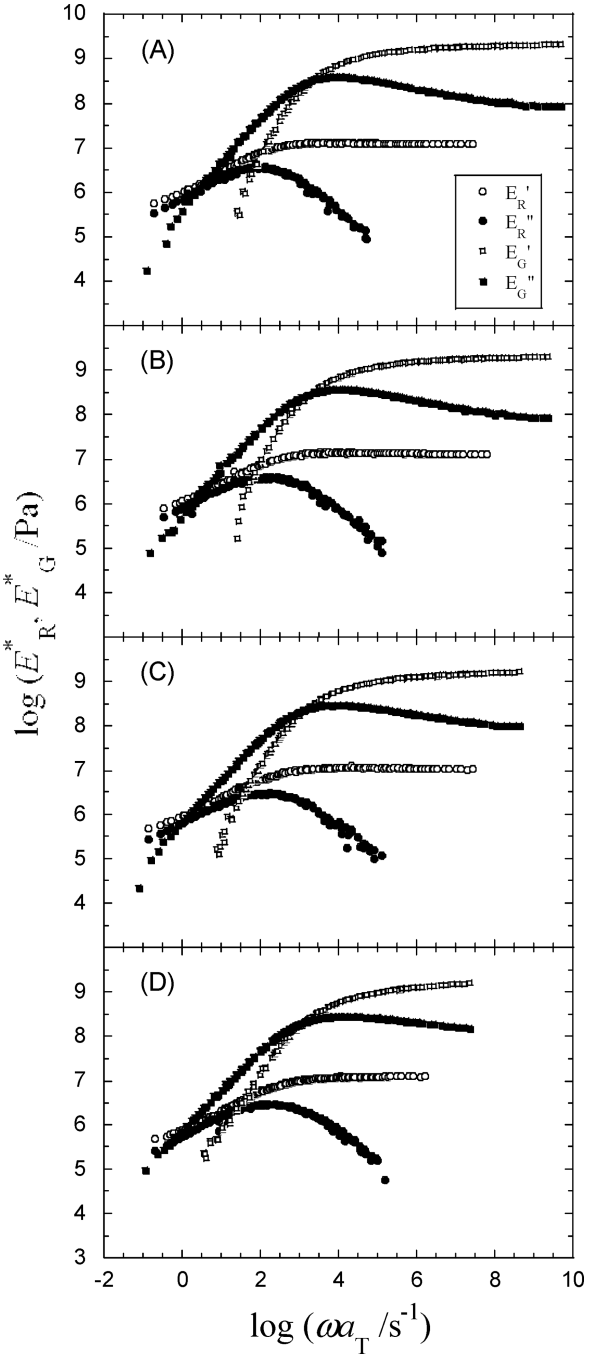

Figure 3. Decomposed rubbery and glassy viscoelastic spectra, E^*_R and E^*_G, respectively, for PS (A) and PS/5CB blend with $W_{5CB} = 0.05$ (B), 0.13 (C), and 0.20 (D) at $T = T_g + 20$ K.

reference temperature was set to be $T_g + 20$K. It is seen that all the shift factors a_T for each mode overlap each other. This means that temperature dependencies of the R and G mode relaxations can be reduced by T_g irrespective of the blend composition. The difference between the two kinds of a_T's (R-and G-modes) is consistent with the data reported by Inoue et al.[38,39]

4.3. Where Does the Rotational Motion of 5CB Appear ? In the previous study,[6,7] we compared the length scales of dynamical unit for 5CB and PS. The average length of the long axis of 5CB is 1.3 nm relevant to the main relaxation (rotational motion) of 5CB, which is slightly smaller than the viscoelastic segmental size of PS, 1.9 nm.[32] The R-mode reflects the large scale motion of polymers (larger than or

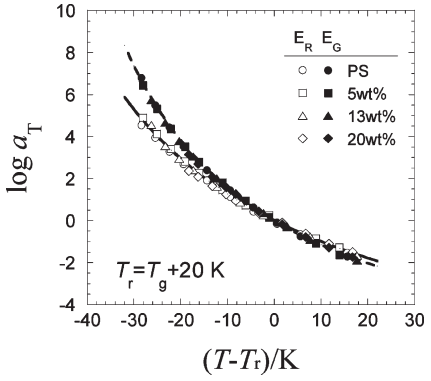

Figure 4. Shift factors of the glass and rubber modes for pure PS and PS/5CB blends as functions of reduced temperature T-T_r with $T_r = T_g$+20K.

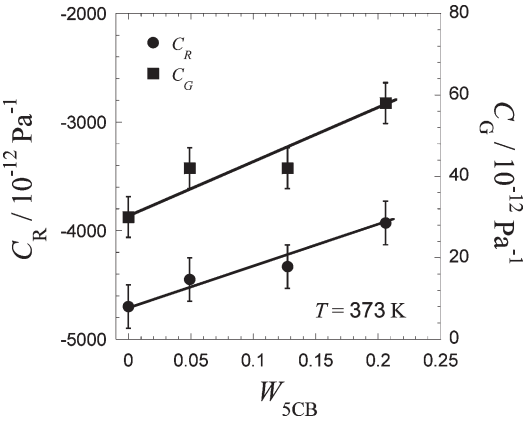

Figure 5. Concentration dependence of C_R and C_G for PS/5CB blends at 373 K.

equal to the size of the viscoelastic segment) and G-mode reflects the motions of the smaller size units than the segment. Therefore, the rotational motion of 5CB will mainly appear in the G-mode. Furthermore, the increase of C_G values with W_{5CB} suggests that the cooperative orientation of the long axis of 5CB with local orientation of PS inside its segment will occur in the G-mode since 5CB has larger intrinsic birefringence than PS. However, we think that the rotational relaxation of 5CB does not complete inside the G-mode and a part of the orientation still remains in the rubber mode due to the NI with the partially orientated (unrelaxed) PS chain.

In the following sections, we will demonstrate that the degree of the residual orientation of 5CB in the R-mode can be evaluated by analyzing the concentration dependence of C_R.

4.4. Concentration Dependence of C_R and C_G. Figure 5 shows the concentration dependence of C_R and C_G. (For pure PS, $C_R = -4.7 \times 10^{-9}$ Pa^{-1} at 373 K and $C_G = 3.2 \times 10^{-11}$ Pa^{-1}. These values agree well with the reported ones.[31]) Both C_R and C_G increase with the 5CB concentration. As mentioned before, polarizability of the long axis of 5CB is larger than that of the short axis and thus the intrinsic birefringence of 5CB is positive. Therefore, the increase of both C_R and C_G with W_{5CB} indicates the orientation of the long axis of 5CB to the stretching direction. As for the increase of C_R (decrease of the absolute value), cooperative orientation of 5CB molecule with PS chain segment through the NI is thought to be the cause. In contrast, the increase of C_G originates from the orientation of 5CB molecule to the stretching direction under (pseudo)affine deformation resulting in an enhancement of the positive

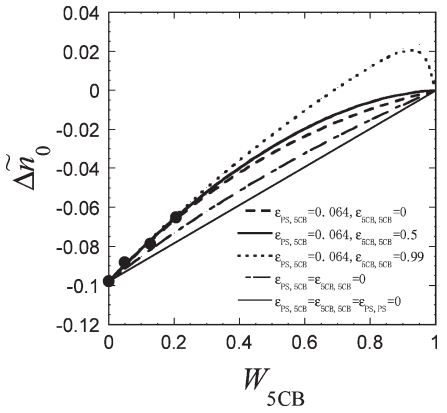

Figure 6. Concentration dependence of Δn_0 for PS/5CB blends. The curves are the calculated results by eq 16 with the parameters indicated in the figure.

birefringence of PS in the G-mode. If 5CB component does not contribute to either stress or birefringence in both modes, just working as a diluent, C_R and C_G will take constant values against W_{5CB}. It is obvious that this is not the case from Figure 5.

4.5. Concentration Dependence of $\Delta\tilde{n}_0$. Figure.6 shows the W_{5CB} dependence of $\Delta\tilde{n}_0$ experimentally determined with eq 15. We approximately regard $W_{5CB} \sim \phi_{5CB}$, since the densities of PS and 5CB are similar. The thin solid line in this figure indicates the proportional relation, i.e., $\Delta n_{0,PS}(1 - \phi_{5CB})$, which corresponds to all NI parameters in eq 16 being zero and means that the dilution of PS chain by mixing 5CB induces the decrease of the absolute value of $\Delta\tilde{n}_0$. It is seen that experimental $\Delta\tilde{n}_0$ value is larger than the thin solid line, indicating the existence of the interaction between PS and 5CB.

In order to fit the data with eq 16, we made the following assumptions to reduce the floating parameters: (1) $\varepsilon_{PS,5CB} \approx \varepsilon_{5CB,PS}$, (2) $x_{PS}/x_{5CB} \sim 1$ (this is a reasonable approximation because densities of PS and 5CB are similar and the sizes of PS segment and 5CB molecule are not so different), and (3) $\varepsilon_{PS,PS} = 0.26$ which was experimentally determined by Tassin et al.[28]

$\Delta n_{0,PS}$ can be related to the C_{PS} ($=-4.7 \times 10^{-9}$ Pa^{-1}) through the eqs 14 and 15, and the formula of $\Delta n_{0,PS} = -0.098 \times (1 - \varepsilon_{PS,PS})$ is obtained including the NI parameter. Concerning the unknown $\Delta n_{0,5CB}$ value, we calculated it from the difference between two polarizabilities in the parallel and perpendicular directions to the long axis of 5CB molecule. The polarizability, P, is given by the Lorentz−Lorenz equation:

$$\frac{n^2-1}{n^2+2}\frac{M}{\rho} = \frac{4}{3}\pi N_A P \tag{18}$$

where n, M, ρ, and N_A are refractive index, molecular weight, density, and Avogadro's number, respectively. Differentiation of eq 18 by P leads to the expression for the intrinsic birefringence, Δn_0, as follows.[36]

$$\Delta n_0 \cong \frac{2}{9}\pi\frac{(n^2+2)^2}{n}\frac{\rho N_A}{M}\Delta P \tag{19}$$

where ΔP is defined as the difference between parallel and perpendicular polarizabilities ($P_\parallel$ and $P_\perp$) to the stretching axis ($\Delta P = P_\parallel - P_\perp$). The ΔP_{5CB} was calculated by using WinMopac software (Fujitsu) and $\Delta n_{0,5CB}$ was determined to be 0.48. It is reported that homogeneously aligned 5CB nematic liquid crystal on the rubbed surface shows birefringence of about 0.21.[42] The orientation of 5CB in the nematic state will not be perfect, and thus the experimental value may be smaller than the calculated one. In this paper we use this calculated value ($\Delta n_{0,5CB} = 0.48$).

Finally eq 16 contains two parameters $\varepsilon_{PS,5CB}$ and $\varepsilon_{5CB,5CB}$. It was found that $\varepsilon_{PS,5CB}$ is much more sensitive than $\varepsilon_{5CB,5CB}$ to the calculated result of $\Delta\tilde{n}_{0,blend}$ at low ϕ_{5CB}. The dotted, thick solid, and dashed curves in Figure.6 demonstrate the calculation results with $\varepsilon_{5CB,5CB} = 0$, 0.5, and 0.99, respectively, at fixed $\varepsilon_{PS,5CB}$ ($= 0.064$). It is seen that the variation of $\varepsilon_{5CB,5CB}$ does not give significant change in $\Delta\tilde{n}_{0,blend}$ at low ϕ_{5CB}. This is because eq 16 at low ϕ_B can be approximated by the following equation:

$$\Delta\tilde{n}_{0,blend} \approx \frac{\phi_A(\Delta n_{0,A} + \phi_B\varepsilon_{A,B}\Delta n_{0,B})}{1 - \phi_A\varepsilon_{A,A}} \tag{20}$$

In contrast, the variation of $\varepsilon_{PS,5CB}$ value is sensitive to the $\Delta\tilde{n}_{0,blend}$ and the optimum value was found. The obtained result was $\varepsilon_{PS,5CB} = 0.070$ ($\varepsilon_{5CB,5CB} = 0$), $\varepsilon_{PS,5CB} = 0.064$ ($\varepsilon_{5CB,5CB} = 0.5$), and $\varepsilon_{PS,5CB} = 0.058$ ($\varepsilon_{5CB,5CB} = 0.99$). The thick solid curve in the figure corresponds to the result using the optimum value. The dash-dotted curve indicates the case of $\varepsilon_{PS,5CB} = 0$ (and $\varepsilon_{5CB,5CB} = 0$). It is seen that the variation of $\varepsilon_{PS,5CB}$ sensitively alter the calculated result. Note that this dash-dotted curve is different from the proportional relation (thin solid line) because the NI between PS−PS, which is weakened with increasing W_{5CB}, is taken into account in this case. From these results we can conclude that intercomponent NI parameter between PS and 5CB ($\varepsilon_{PS,5CB}$) can be determined to be 0.064 with ±10% accuracy.

The determined $\varepsilon_{PS,5CB}$ ($=0.064$) is about a quarter of $\varepsilon_{PS,PS}$ ($=0.26$),[28] which was determined through the infrared absorption dichroism measurements for blends of low molecular weight deuterated PS with high molecular weight PS. This indicates the weaker nematic interaction acting between PS-5CB than between PS-dPS, suggesting that dynamically homogeneous behavior of PS/5CB system[6,7] is not directly related to the NI between the components. As we described as "speculation" in the introduction, we can say that strong NI is not required for the cooperative component dynamics. The origin of the dynamic homogeneity in PS/5CB blends might be in the large size of 5CB molecules. In the previous study, we demonstrated the existence of the critical size above which the LM dynamics became cooperative with that of PS segments.

From a practical viewpoint, small $\varepsilon_{PS,5CB}$ value indicates that 5CB cannot effectively compensate the birefringence of PS. As can be seen in eq 20, if $\Delta n_{0,A}$ and $\Delta n_{0,B}$ have opposite signs and $\varepsilon_{A,B}$ is large enough, the birefringence of the mixture can become zero even at lower LM concentration. This means that intercomponent NI parameter $\varepsilon_{A,B}$ as well as the intrinsic birefringence of each component plays an significant role in controlling the polymer birefringence by mixing LMs. Actually, eq 20 indicates that the product of $\varepsilon_{A,B}\Delta n_{0,B}$ determine the $\Delta\tilde{n}_{0,blend}$. Therefore, the evaluation of $\varepsilon_{A,B}$ is important not only in newly creating zero-birefringent polymer/LM mixtures but also in understanding already reported results for such mixtures in which only the intrinsic birefringence values of the components have been mainly focused on.[29]

The small $\varepsilon_{PS,5CB}$ value suggests that NI strength depends on the chemical structure: NI between different chemical species might be weak. The difference in the shapes and/or sizes between PS segments and 5CB molecules will also be a possible origin for the small value of $\varepsilon_{PS,5CB}$. As a future

problem it will be necessary to consider the correlation between the chemical structure and the ε_{AB} value.

5. Conclusions

We made simultaneous measurements of dynamic birefringence and viscoelastic relaxation for PS/5CB blend. By applying the MSOR, C_R and C_G values were determined as functions of 5CB concentration. The C_R value was negative and increased (absolute value of C_R decreased) with increasing 5CB concentration, indicating the partial orientation of the mesogenic low-mass molecules to the orientation direction of PS segments through the nematic interaction (NI).

We determined intercomponent NI parameter in PS/5CB blends using a newly proposed equation. The NI parameter, $\varepsilon_{PS,5CB}$, was 0.064 ± 0.006 being smaller compared with the value of $\varepsilon_{PS,PS}$ (0.26). The weak NI between PS and 5CB suggested that NI strength between different components in miscible mixtures depends on their chemical structures including the size and/or shape differences. From the result that the NI parameter was small in the dynamically homogeneous blend, we concluded that there is no direct correlation between dynamic cooperativity and orientational coupling.

The derived equations in this paper (eqs16 and 20) indicated that the larger $\varepsilon_{A,B}$, the more effectiveness to control the birefringence of the mixture. This means that the determination of $\varepsilon_{A,B}$ is very important in creating zero-birefringent polymer/LM mixtures.

Acknowledgment. This work was partly supported by the Osaka University Global COE program, "Global Education and Research Center for Bio-Environmental Chemistry" from the Ministry of Education, Culture, Sports, Science, and Technology, Japan, and by Grant-in-Aid for Scientific Research B from the Japan Society for the Promotion of Science (Grant Nos. 1806809, 20340112, and 21350126).

References and Notes

(1) Ferry, J. D. *Viscoelastic Properties of Polymers*, 3rd ed.; Wiley: New York, 1980.
(2) Adachi, K.; Fujihara, I.; Ishida, Y. *J. Polym. Sci., Polym. Phys. Ed.* **1975**, *13*, 2155–2171.
(3) Yoshizaki, K.; Urakawa, O.; Adachi, K. *Macromolecules* **2003**, *36*, 2349–2354.
(4) Taniguchi, N.; Urakawa, O.; Adachi, K. *Macromolecules* **2004**, *37*, 7832–7838.
(5) Hori, H.; Urakawa, O.; Adachi, K. *Polym. J* **2003**, *35*, 721–727.
(6) Urakawa, O.; Ohta, E.; Hori, H.; Adachi, K. *J.Polym.Sci.: Part B* **2006**, *44*, 967–974.
(7) Urakawa, O.; Nobukawa, S.; Shikata, T.; Inoue, T. *Nihon Reoroji Gakkaishi* **2010**, *38*, 41–46.
(8) Nobukawa, S.; Urakawa, O.; Shikata, T.; Inoue, T. *AIP Conf. Proc.* **2008**, *1027*, 561–563.
(9) Colby, R. H. *Polymer* **1989**, *30*, 1275–1278.
(10) Chung, G. C.; Kornfield, J. A.; Smith, S. D. *Macromolecules* **1994**, *27*, 964–973.
(11) Chung, G. C.; Kornfield, J. A.; Smith, S. D. *Macromolecules* **1994**, *27*, 5729–5741.
(12) Alegria, A.; Colmenero, J.; Ngai, K. L.; Roland, C. M. *Macromolecules* **1994**, *27*, 4486–4492.
(13) Leroy, E.; Alegria, A.; Colmenero, J. *Macromolecules* **2002**, *35*, 5587–5590.
(14) Urakawa, O.; Fuse, Y.; Hori, H.; Tran-Cong, Q.; Yano, O. *Polymer* **2001**, *42*, 765–773.
(15) Hirose, Y.; Urakawa, O.; Adachi, K. *Macromolecules* **2003**, *36*, 3699–3708.
(16) Lutz, T. R.; He, Y. Y.; Ediger, M. D.; Cao, H. H.; Lin, G. X.; Jones, A. A. *Macromolecules* **2003**, *36*, 1724–1730.
(17) Haley, J. C.; Lodge, T. P.; He, Y.; Ediger, M. D.; Von Meerwall, E. D.; Mijovic, J. *Macromolecules* **2003**, *36*, 6142–6151.
(18) Haley, J. C.; Lodge, T. P. *Colloid Polym. Sci.* **2004**, *282*, 793–801.
(19) Urakawa, O.; Ujii, T.; Adachi, K. *J. Non-Cryst. Solids* **2006**, *352*, 5042–5049.
(20) Colmenero, J.; Arbe, A. *Soft Matter* **2007**, *3*, 1474−1485, and references therein.
(21) Watanabe, H.; Urakawa, O. *Kor.-Australia Rheol. J.* **2009**, *21*, 235−244, and references therein.
(22) Lodge, T. P.; Mcleish, T. C. B. *Macromolecules* **2000**, *33*, 5278–5284.
(23) Doi, M.; Pearson, D.; Kornfield, J.; Fuller, G. *Macromolecules* **1989**, *22*, 1488–1490.
(24) Watanabe, H.; Kotaka, T.; Tirrell, M. *Macromolecules* **1991**, *24*, 201–208.
(25) Doi, M.; Watanabe, H. *Macromolecules* **1991**, *24*, 740–744.
(26) Kornfield, J. A.; Fuller, G. G.; Pearson, D. S. *Macromolecules* **1989**, *22*, 1334–1345.
(27) Zawada, J. A.; Fuller, G. G.; Colby, R. H.; Fetters, L. J.; Roovers, J. *Macromolecules* **1994**, *27*, 6851–6860.
(28) Tassin, J.-F.; Baschwitz, A.; Moise, J.-Y.; Monnerie, L. *Macromolecules* **1990**, *23*, 1879–1881.
(29) Tagaya, A.; Iwata, S.; Kawanami, E.; Tsukahara, H.; Koike, Y. *Appl. Opt.* **2001**, *40*, 3677–3683.
(30) Saito, H.; Inoue, T. *J. Polym. Sci.: Part B* **1987**, *25*, 1629–1636.
(31) Inoue, T.; Okamoto, H.; Osaki, K. *Macromolecules* **1991**, *24*, 5670–5675.
(32) Inoue, T.; Mizukami, Y.; Okamoto, H.; Matsui, H.; Watanabe, H.; Kanaya, T.; Osaki, K. *Macromolecules* **1996**, *29*, 6240–6245.
(33) Inoue, T. *Nihon Reoroji Gakkaishi* **2000**, *28*, 167–175.
(34) Inoue, T.; Matsui, H.; Osaki, K. *Rheol. Acta* **1997**, *36*, 239–244.
(35) Ward, I. M. *J. Polym. Sym* **1977**, *58*, 1–21.
(36) Oh, G.-K.; Inoue, T. *Rheol. Acta* **2005**, *45*, 116–123.
(37) Plazek, D. J. *J. Phys. Chem.* **1965**, *69*, 3480–3487.
(38) Inoue, T.; Onogi, T.; Yao, M.-L.; Osaki, K. *J. Polym. Sci., Part B: Polym. Phys.* **1999**, *37*, 389–397.
(39) Inoue, T.; Onogi, T.; Osaki, K. *J. Polym. Sci., Part B: Polym. Phys.* **2000**, *38*, 954–964.
(40) According to rubber elasticity theory,[41] the stress, σ_R, in the rubbery state is proportional to T, while the corresponding (strain-induced) birefringence, Δn_R, in the same state is independent of T. Therefore, C_R ($= \Delta n_R/\sigma_R$) should be inversely proportional to T.
(41) Doi, M.; Edwards, S. F. *The Theory of Polymer Dynamics*: Oxford University Press: New York, 1986.
(42) Koysal, O.; San, S. E.; Ozder, S.; Ecevit, F. N. *Meas. Sci. Technol* **2003**, *14*, 790–795.